Real-time optical imaging of experimental brain ischemia and hemorrhage in neonatal piglets

Miljan R. Stankovic[1, 4, 5], Dev Maulik[1], Warren Rosenfeld[2], Phillip G. Stubblefield[4], Alexander D. Kofinas[5], Steven Drexler[3], Ramesh Nair[3], Maria Angela Franceschini[6], Dennis Hueber[7], Enrico Gratton[6], and Sergio Fantini[6]

[1]Departments of Obstetrics and Gynecology, [2]Pediatrics, and [3]Pathology, Winthrop University Hospital, State University of New York at Stony Brook, Mineola, NY, [4]Department of Obstetrics and Gynecology, Boston University School of Medicine, Boston, MA, [5]Department of Obstetrics and Gynecology, Brooklyn Hospital Center, Cornell University School of Medicine, Brooklyn, NY, [6]Laboratory for Fluorescence Dynamics, Department of Physics, University of Illinois at Urbana-Champaign, Urbana, IL, and [7]ISS Inc., Champaign, IL, USA

1 Introduction

Perinatal hypoxic-ischemic brain injury with or without brain hemorrhage is a major cause of perinatal neurological morbidity and mortality leading to cerebral palsy, mental retardation, and seizures [15]. Studies in humans and animals have demonstrated the importance of disturbances in cerebral hemodynamics and oxygenation in the pathogenesis of perinatal brain injury [22]. Early identification and treatment of these disturbances, as well as the detection of brain ischemia and hemorrhage, may improve neurological outcome [22]. To achieve this, continuous monitoring of cerebral hemodynamics and oxygenation is required [22, 20].

Near infrared spectroscopy (NIRS) can provide this type of information non-invasively and real time [13]. NIR light can penetrate through the intact scalp and skull up to several centimeters deep into the brain and measure concentrations of oxyhemoglobin and deoxyhemoglobin, the two major absorbers in the NIR range. Several groups have demonstrated use of NIRS to measure changes in brain concentrations of oxyhemoglobin and deoxyhemoglobin associated with different physiological conditions [13, 16].

Optical brain imaging, merging the features of both spectroscopy (temporal information) and tomography (spatial information), has already been successfully used in the detection of neonatal brain hemorrhage in humans and animals [21, 11, 12, 18]. Unfortunately, the previously reported image-acquisition times ranging from 5 s [18] to several hours [11, 12], or even days [21] were far too slow to allow for real-time imaging.

To prove the hypothesis that brain ischemia and hemorrhage can be imaged in real-time with good spatial and temporal resolution, a prototype imager was used in a newborn piglet model. Cerebral ischemia and hemorrhage were induced by the direct injections of saline and blood into the left subcortical brain region. From the optical standpoint, a focal decrease in absorption associated with the appearance of saline simulates brain ischemia, while the appearance of blood causes a focal increase in brain absorption consistent with the formation of brain hematoma. The increase in intracranial pressure associated with volume injections induces global decrease in brain absorption in the surrounding ipsilateral and contralateral brain that is consistent with brain ischemia.

2 Methods

2.1 Animal model

The study was approved by the Institutional Review Board at Winthrop University Hospital, Mineola, NY. A newborn piglet model of cerebral ischemia and hemorrhage using stereotaxic injection of saline and blood into the left subcortical region was developed. A total of seven 10.7 $\pm$ 1.9 day old newborn piglets of either sex, weighing 2.6 $\pm$ 0.3 kg were sedated with ketamine 20 mg/kg mixed with xylazine 4 mg/kg, i.m., intubated, and ventilated with an infant ventilator (Bear Medical Systems Inc., Riverside, CA) to achieve normal blood gas values. General anesthesia was maintained by a continuous infusion of propofol mixed in D5W at a concentration of 0.8 mg/ml at 4$-$8 mg/kg/hr. The core temperature was maintained at 37 °C with the use of a heating blanket and continuously monitored by a rectal thermometer. A femoral cut-down was performed and the femoral artery was catheterized. The catheter was advanced into the abdominal aorta for continuous blood pressure monitoring (Hewlett Packard 78353B, USA) and arterial blood gas analyses (Ciba $-$ Corning 238 pH $-$ Blood Gas Analyzer, Medfield, MA). The femoral vein was catheterized and the catheter was advanced into the inferior vena cava for continuous infusion of D5W and propofol. Heart rate and arterial oxygen saturation were monitored by pulse oximetry (Nellcor Inc, Hayward, CA) with the probe attached to the pig's tail. To achieve a motion-artifact-free imaging environment and reproducible brain hematomas, the pre-shaved animal's head was secured within a stereotaxic instrument (Lab Standard 51600, Stoelting, Wood Dale, IL) with two 18° ear bars and a nose clamp. The manipulator arm of the stereotaxic instrument allowed for: 1) drilling a hole in the skull in precise stereotaxic coordinates, 2) three-dimensional positioning of the optical probe, and 3) optimal probe-to-scalp contact. A 25¾ G needle was inserted through the skull hole placed in the left frontal region, and advanced into the left frontal subcortical white matter to a depth of 0.8 cm from the surface of the brain. A total of 0.3 cc of normal saline (contained within the 30 cm long tubing connecting the needle and the injection set), followed by 2 cc of autologous blood, was injected over a period of $\sim$ 40 s. No

resuscitation was required at any time. The piglets were sacrificed by an overdose of sodium pentobarbital. An autopsy was performed to determine the type, size, and location of the hemorrhage, and to validate optical data.

2.2 Optical imaging

The basic principles of NIRS [24, 16, 20] and optical imaging [4, 5, 2, 3, 1, 7] are well described in the literature. Optical imaging was performed with a modified dual channel frequency domain tissue oximeter (Model 96208, ISS Inc., Champaign, IL) [9]. The instrument uses eight light sources emitting at 758 nm and eight at 830 nm. The 16 light sources (laser diodes) and two optical detectors (photomultiplier tubes) are all coupled to optical fibers, which guide the light to and from the piglet head respectively. The light sources were electronically multiplexed, so that they were turned on and off in sequence every 12 ms. Consequently, the acquisition time was 192 ms per image (16 diodes $\times$ 12 ms/diode) allowing for real-time imaging. Imaging was performed by arranging 16 source fibers and 2 detector fibers over an area of 5 $\times$ 5 cm (figure 1A) resembling that of the piglet brain. The photons emitted at the multiple source locations (figure 1B) were collected by the detector fibers. The imager measures the time evolution of attenuation of the detected light. The dc (direct current) intensity data collected by each of the source-detector pairs was translated into a variation in the absorption coefficient by using the differential pathlength factor (DPF) method [8]. DPF values for the newborn piglet brain used to calculate the absorption coefficient were measured with frequency domain spectroscopy using the expression for the DPF predicted by the diffusion theory in a semi-infinite medium [9]. In the range of source-detector distances featured in the imaging probe (1.8$-$2.5 cm), we found DPF values ranging from 5.3 to 5.7. Finally, the absorption data calculated for each source-detector pair was back-projected to generate 64 pixel / 4 $\times$ 4 cm / 2-D absorption images of the brain (figure 2). The back-projection scheme is based on: 1) assigning each source-detector reading to the pixels between the source and the detector (along the banana-shaped region visited by the
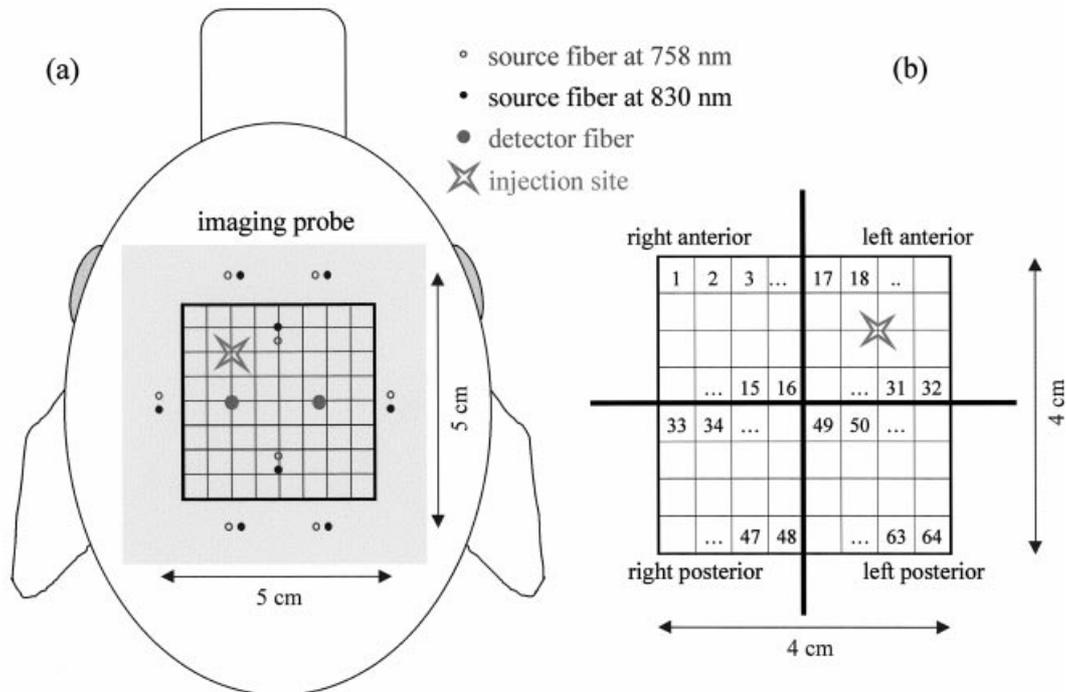
Figure 1. Imaging probe (A). Optical fibers are arranged to generate 4 cm X 4 cm / 64-pixel images (B).

detected photons), and 2) averaging the multiple readings corresponding to more than one source-detector pair [2, 3].

In order to emphasize temporal and spatial aspects of the cerebral absorption changes associated with volume injections, as well as to demonstrate the reproducibility between different subjects, the 64 − pixel images were divided into four quadrants, each containing 16 pixels (figure 1B). The absorption values for each of the quadrants (figure 2, right anterior, right posterior, left anterior, and left posterior) were averaged (mean ± SD) and plotted over time (figure 3). The sensitivity of the imager to detect blood or saline in the brain was defined as the volume of the injected blood or saline causing a change in measured intensity greater than 3 times the SD of the baseline intensity.

3   Results

The imager detected 2 subarachnoid hemorrhages with small subcortical hematomas and 5 subcorti-

cal hematomas rendered by blood injections, as confirmed on autopsy. Images from 2 to 8 show the appearance and then a gradual increase in the volume of saline in the left anterior (LA) region of the brain. Images from 9 to 17 show the appearance and then a gradual increase in the volume of blood in the left anterior (LA) region of the brain (figure 2). Image 18 is a photograph of a brain section at the hematoma level obtained post mortem from a pig that developed a subcortical hematoma (figure 2). As the injected blood acted as a perfect optical absorber, the optical recordings were similar at both wavelengths (758 and 830 nm). Therefore, the oxygen saturation of the hematoma was immeasurable. For that reason only the 830-nm images were presented (figure 2). However, the optical changes obtained from the surrounding ipsilateral and contralateral brain at two wavelengths were different (the comparison between the images obtained at different wavelengths, from different tissues, and during different conditions will be presented in a separate publication). The instrument revealed a generalized decrease in brain absorption (every
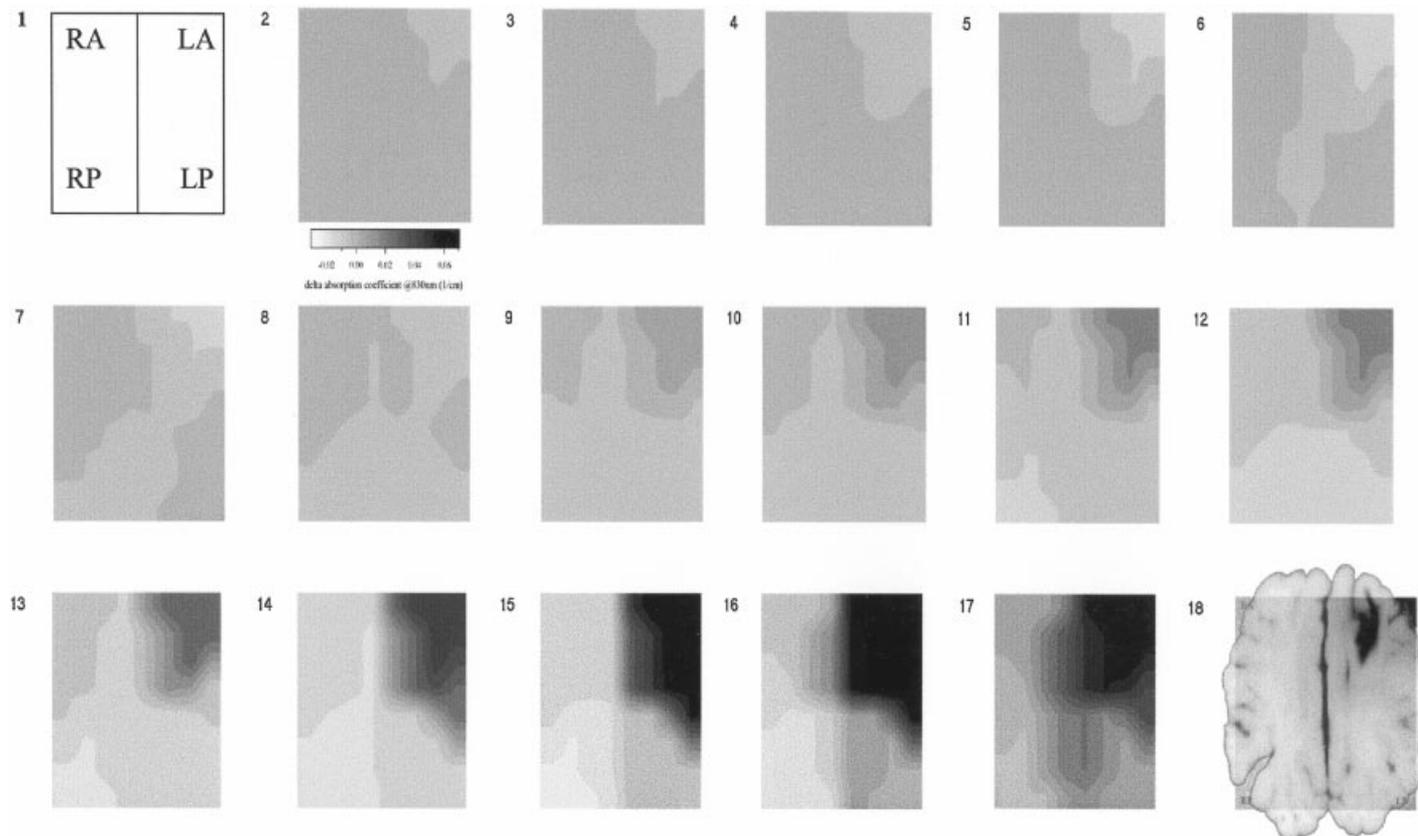
Figure 2. Optical images of brain ischemia and hemorrhage. Images 2–8 show the injection of saline, images 9–17 show the injection of blood. A total of 0.3 cc of saline followed by 2 cc of blood was injected into the left anterior brain subcortical white matter. LA = left anterior, LP = left posterior, RA = right anterior, RP = right posterior. The appearance of saline caused a local decrease in brain absorption (light gray area) at the injection site (LA) (images 2–8). The presence of blood caused the opposite effect, i. e., a local increase in absorption (dark gray and black areas) at the injection site (LA) (images 9–18). Both saline and blood injections caused ischemic changes (associated with the increase in intracranial pressure) in the surrounding ipsilateral, as well as in the contralateral brain (light gray or white areas) (images 6–17). Image 18 is a photograph of a brain section at the hematoma level obtained *post mortem* from a piglet that developed subcortical hematoma. Image #8 = 0.3 cc of saline, image #10 = 0.25 cc of blood, image #12 = 0.5 cc of blood, image #13 = 1.0 cc of blood, image #14 = 1.5 cc of blood, and image #17 = 2.0 cc of blood.
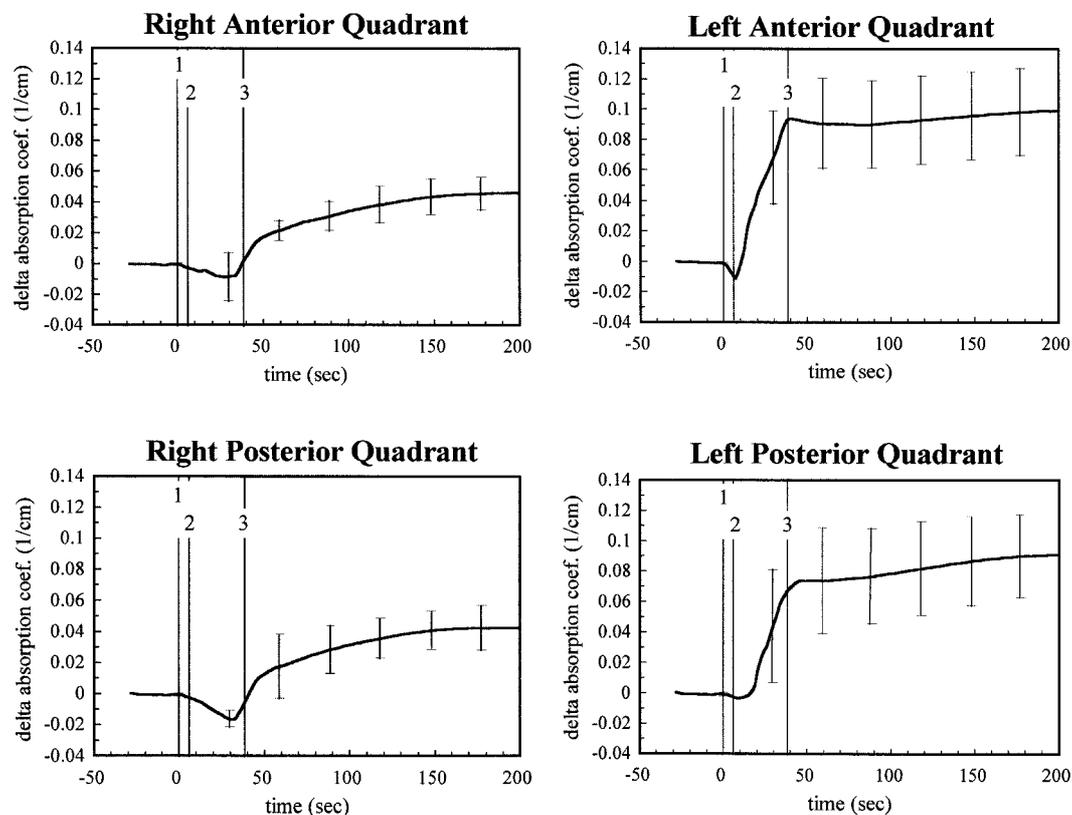
Right Anterior Quadrant

Left Anterior Quadrant

Right Posterior Quadrant

Left Posterior Quadrant

Figure 3. Regional (quadrant) changes in cerebral absorption at 830 nm associated with subcortical injections of 0.3 cc of saline and 2 cc blood obtained from 5 newborn pigs. Vertical lines indicate the time when the instrument first detected the presence of saline (line 1) and blood (line 2), as well as the end of blood injection at the injection site (line 3 / LA quadrant). The increase in absorption in the left posterior (LP) brain quadrant at ∼ 10 sec suggests a posterior expansion of the hematoma. At the same time, the absorption in the contralateral (RA and RP) brain quadrants continued to decline, suggesting brain ischemia.

decrease in brain absorption is consistent with brain ischemia [16, 17]) caused by the accompanying increase in intracranial pressure in the surrounding ipsilateral (figure 3-LP) and contralateral brain (figure 3 / RA and RP). These intracranial-pressure-related ischemic changes can be seen in optical images presented in figure 2 (images 6 − 18). Once the injection was terminated (figure 3 − line 3), the ischemic changes in the ipsilateral (LP) and contralateral (RA and RP) brain recovered (the period of reperfusion) followed by an overshoot (the period of hyperemia). The detection threshold at the estimated depth of 1 − 1.5 cm was 0.07 cc for saline and 0.04 cc for blood.

4 Discussion

This study presents a successful application of optical imaging in the detection of experimental brain ischemia and hemorrhage and the accompanying cerebrovascular changes in newborn piglets. Near infrared spectroscopy (NIRS) is based on the ability of NIR light to non-invasively penetrate intact scalp and skull and measure brain concentrations of oxyhemoglobin and deoxyhemoglobin. As oxy- and deoxyhemoglobin are the two major absorbers in the NIR region, changes in brain absorption can be attributed to changes in hemoglobin concentration [6].

The animal model based on the injections of blood and saline has shown to be a good model for studying brain ischemia and hemorrhage. Similar blood injection models have been described in rat [19] and piglets [23, 18]. The appearance of blood caused a focal increase in brain absorption accompanying the formation of the hematoma. These results are consistent with the previously reported increase in brain absorption associated with the formation of intracranial hematoma [10]. The appearance of saline caused the opposite effect, i. e. a focal decrease in absorption consistent with brain ischemia [16, 17, 20]. As hemoglobin is a dominant brain tissue absorber, any decrease in brain absorption is an equivalent to brain ischemia [16, 17, 20]. The increase in intracranial pressure associated with both saline and blood injections caused global decrease in brain absorption in the surrounding ipsilateral and contralateral brain, consistent with brain ischemia [16, 17, 20]. These results are consistent with the previously reported decrease in brain absorption (decrease in total hemoglobin concentration) associated with brain ischemia caused by different factors, as confirmed by carotid Doppler [16, 17] and radioactive-labeled microspheres [20].

Spatial and temporal resolution are the two major features defining the successful performance of any imaging technique. While NIRS can provide only global information on hemoglobin concentration (changes), optical imaging − merging the features of NIRS (temporal information) and tomography (spatial information) can address regional differences in brain absorption. This study has confirmed the capability of optical imaging in detecting small intracranial optical inhomogeneities in the brain with the high detection thresholds for both saline and blood at the esti-

mated depth of 1−1.5 cm. These results are consistent with the previously reported detection thresholds of 0.05 cc of blood obtained with a different continuous wave imager and a 16 − source − 9 − detector optical probe used in a similar blood injection piglet model [18]. The results are also consistent with the detection threshold of 3 mm at a depth of 2 cm, and 1 cm at a depth of 5 cm obtained with a time-of-flight imager in pathologic brain specimens [21] and human newborns [11, 12]. Although the spatial resolution of optical imaging is intrinsically limited by multiple scattering to several millimeters [11], a finer distribution and higher density of source-detector pairs would reduce the pixel size and increase the resolution of optical images.

This is, to our knowledge, the first report on real-time optical imaging. The acquisition rate of 5.26 images per sec that we used for this study allowed for real-time imaging of the developing brain hemorrhage, ischemia, and reperfusion with high temporal resolution. Previously reported acquisition times of 5 sec [18], 1−6 hours [11, 12], or even 1 to 3 days per image [21] were far too slow to allow for real-time imaging. Real-time information would be particularly important in neonatal settings where acute events are the focus of our attention, and where the images can be degraded by motion artifacts.

Although this work demonstrates the potentials of optical imaging, significant research and development is anticipated before this technique becomes a useful clinical tool. This research is important now when a wide variety of therapeutic strategies are in use aiming to reduce perinatal neurological morbidity and mortality [14]. Monitoring of their efficacy, and side effects on cerebral perfusion and oxygenation, would be very important.

Abstract

Our objective was to study the development of experimental brain ischemia and hemorrhage by real-time optical imaging. Optical imaging is based on the ability of near infrared light to non-invasively penetrate through the intact scalp and skull and measure brain concentrations of oxy- and deoxyhemoglobin, dominant brain absorbers. Optical imaging was performed in 7 anesthetized, instrumented, and ventilated newborn piglets subjected to the injection of 0.3 cc of saline followed by 2 cc of blood into the left frontal subcortical brain re-

gion via a needle inserted through the skull with stereotactic guidance. The image-acquisition rate of 5.26 images per sec allowed for real-time imaging. The detection threshold of the imager at the estimated depth of 1−1.5 cm was ∼ 70 μL for saline and ∼ 40 μL for blood. The imager readily detected five subcortical hematomas and two large bilateral subarachnoid hemorrhages. The imager detected a global decrease in brain absorption associated with the volume-injection-related increase in intracranial pressure in the surrounding ipsi-

lateral and contralateral brain. Any decrease in brain absorption is an equivalent to brain ischemia. This study demonstrates the capability of optical imaging in detecting brain ischemia and hemorrhage in real-time with high temporal and spatial resolution.

Keywords: Brain hemorrhage, brain ischemia, near infrared spectroscopy, newborn piglet, optical imaging.

References

[1] Alfano RR, SG Demos, P Galland, SK Gayen, Y Guo, PP Ho, X Liang, F Liu, L Wang, QZ Wang, WB Wang: Time-resolved and nonlinear optical imaging for medical applications. Ann N Y Acad Sci 838 (1998) 14

[2] Arridge SR, JC Hebden: Optical imaging in medicine: II. Modelling and reconstruction. Phys Med Biol 42 (1997) 841

[3] Arridge SR, M Schweiger: Image reconstruction in optical tomography. Philos Trans R Soc Lond B Biol Sci 352 (1997) 717

[4] Benaron DA, WE Benitz, RA Ariagno, DK Stevenson: Noninvasive methods for estimating in vivo oxigenation. Clinical Pediatrics 31 (1992) 258

[5] Chance B, K Kang, L He, J Weng, E Sevick: Highly sensitive object location in tissue models with linear in-phase and anti-phase multi-element optical arrays in one and two dimensions. Proc Natl Acad Sci USA 90 (1993) 3423

[6] Chance B, Q Luo, S Nioka, DC Alsop, JA Detre: Optical investigations of physiology: a study of intrinsic and extrinsic biomedical contrast. Philos Trans R Soc Lond B Biol Sci 352 (1997) 707

[7] Cheng X, MR Stankovic, PG Stubblefield, DA Boas: An investigation of the effects of layered tissue on NIR imaging of deep heterogenous structure. In: Advances in Optical Imaging and Photon Migration. Orlando FL 1998

[8] Delpy DT, M Cope, P van der Zee et al: Estimation of optical pathlength through tissue from direct time of flight measurement. Phys Med Biol 33 (1988) 1433

[9] Fantini S, D Hueber, MA Franceschini, E Gratton, W Rosenfeld, PG Stubblefield, D Maulik, MR Stankovic: Non-invasive optical monitoring of the newborn piglet brain using continuous wave and frequency domain spectroscopy. Phys Med Biol (1999) (in press)

[10] Gopinath SP, CS Robertson, CF Contant, RK Narayan, RG Grossman, B Chance: Early detection of delayed traumatic intracranial hematomas using near-infrared spectroscopy. J Neurosurg 83 (1995) 438

[11] Hintz SR, DA Benaron, JP van Houten, JL Duckworth, FW Liu, SD Spilman, DK Stevenson, WF Cheong: Stationary headband for clinical time-of-flight optical imaging at the bedside. Photochem Photobiol 68 (1998) 361

[12] Hintz SR, WF Cheong, JP van Houten, DK Stevenson, DA Benaron: Bedside imaging of intracranial hemorrhage in the neonate using light: comparison with ultrasound, computed tomography, and magnetic resonance imaging. Pediatr Res 45 (1999) 54

[13] Hirtz DG: Report of the National Institute of Neurological Disorders and Stroke workshop on near infrared spectroscopy. Pediatrics 91 (1993) 414

[14] Maulik D, S Zanelli, Y Numagami, ST Ohnishi, OP Mishra, M Delivoria-Papadopoulos: Oxygen free radical generation during in-utero hypoxia in the fetal guinea pig brain: the effects of maturity and of magnesium sulfate administration. Brain Res 817 (1−2) (1999) 117

[15] Nelson KB, JH Ellenberg: Antecedents of cerebral palsy: Multivariate analysis of risk. N Engl J Med 315 (1986) 8

[16] Stankovic MR, A Fujii, D Maulik, D Boas, D Kirby, PG Stubblefield: Optical monitoring of cerebral hemodynamics and oxygenation in the neonatal piglet. J Maternal Fetal Invest 8 (1998) 71

[17] Stankovic MR, A Fujii, D Maulik, D Kirby, PG Stubblefield: Optical brain monitoring of the cerebrovascular effects induced by the acute cocaine exposure in neonatal pigs. J Maternal Fetal Invest 8 (1998) 108

[18] Stankovic MR, D Maulik, A Siegel, W Rosenfeld, PG Stubblefield, D Boas: Optical brain monitoring and imaging in the fetus and neonate. J Fertil Reprod 2 (1998) 18

[19] Thulborn KR, AG Sorensen, NW Kowall, A McKee, A Lai, RC McKinstry, J Moore, BR Rosen, TJ Brady: The role of ferritin and hemosiderin in the MR appearance of cerebral hemorrhage: a histopathologic biochemical study in rats. AJR Am J Roentgenol 154 (1990) 1053

[20] Tsuji M, A duPlessis, G Taylor, R Crocker, JJ Volpe: Near infrared spectroscopy detects cerebral ischemia during hypotension. Pediatr Res 44 (1998) 591

[21] van Houten JP, DA Benaron, S Spilman, DK Stevenson: Imaging brain injury using time resolved near infrared light scanning. Pediatr Res 39 (1996) 470

[22] Volpe JJ: Neurology of the Newborn. WB Saunders, Philadelphia [3]/1995

[23] Wagner KR, G Xi, Y Hua, M Kleinholz, GM Courten-Myers, RE Myers, JP Broderick, TG Brott: Lobar intracerebral hemorrhage model in pigs: Rapid edema development in perihematomal white matter. Stroke 27 (1996) 490

[24] Wahr JA, KK Temper, S Samra, DT Delpy: Near-infrared spectroscopy: Theory and applications. J Cardiothoracic and Vascular Anesthesia 3 (1996) 406

Miljan R. Stankovic, MD, Ph.D.
Department of Obstetrics and Gynecology
The Brooklyn Hospital Center
121 Dekalb Avenue
Brooklyn NY 11201
USA
Tel: +1 (718) 250−6930
Fax: +1 (718) 250−8881
e-mail: MILJANRS@AOL. COM